Phys. Status Solidi C **8**, No. 3, 759–762 (2011) / **DOI** 10.1002/pssc.201000334

physica status solidi c
www.pss-c.com
*current topics in solid state physics*

# Enhanced iron gettering by short, optimized low-temperature annealing after phosphorus emitter diffusion for industrial silicon solar cell processing

**Jasmin Hofstetter[*,1], Jean-François Lelièvre[2], David P. Fenning[3], Mariana I. Bertoni[3], Tonio Buonassisi[3], Antonio Luque[1], and Carlos del Cañizo[1]**

[1] Universidad Politécnica de Madrid, Avd. Complutense s/n, 28040 Madrid, Spain
[2] Centro de Tecnología del Silicio Solar, *CENTESIL*, Madrid, Spain
[3] Massachusetts Institute of Technology, Cambridge, MA 02139, USA

Received 13 May 2010, revised 22 July 2010, accepted 6 August 2010
Published online 25 January 2011

**Keywords** P gettering, simulation, silicon solar cells, defect engineering

[*] Corresponding author: e-mail jasmin.hofstetter@ies-def.upm.es, Phone: +34-914533549, Fax: +34-915446341

The introduction of a low-temperature (LT) tail after P emitter diffusion was shown to lead to considerable improvements in electron lifetime and solar cell performance by different researchers. So far, the drawback of the investigated extended gettering treatments has been the lack of knowledge about optimum annealing times and temperatures and the important increase in processing time. In this manuscript, we calculate optimum annealing temperatures of Fe-contaminated Si wafers for different annealing durations. Subsequently, it is shown theoretically and experimentally that a relatively short LT tail of 15 min can lead to a significant reduction of interstitial Fe and an increase in electron lifetime. Finally, we calculate the potential improvement of solar cell efficiency when such a *short-tail extended* P diffusion gettering is included in an industrial fabrication process.



**1 Introduction** In the course of reducing the cost of photovoltaic energy, cheaper solar grade silicon materials of lower purity are being developed. Moreover, about 50% of mc-Si wafers originate from the ingot edge and corner regions containing higher amounts of impurities, mainly Fe [1,2]. The use of these materials demands a more effective impurity reduction during solar cell processing to maintain or even increase solar cell efficiencies.

It was shown by different researchers that low-temperature annealing (LTA) after P-diffusion (PD) can lead to higher charge carrier lifetimes and thus, to better device performance [3–5]. As an example, Rinio *et al.* [5] achieved an absolute efficiency increase of up to 0.8% for LTA at 500 ° during several hours. The drawback of these investigated *extended* gettering treatments is the long extra-processing time required to achieve noticeable improvements. So far, the optimum annealing time and temperature were unknown parameters and their experimental optimization is a time- and cost-intensive task.

In the present work, we show that an enhanced reduction of the interstitial Fe concentration, [$Fe_i$], and an appreciable increase in electron lifetimes can yet be achieved adding a short LT tail of 15 min to standard PD when the appropriate temperature is chosen. With our newly developed Impurity-to-Efficiency (I2E) simulation tool [6], we are able to simulate the evolution of the Fe distribution during solar cell processing and to translate the final Fe distribution into minority carrier lifetimes and solar cell efficiency. First experimental results confirm that a *short-tail extended* P diffusion gettering (PDG) bears a great potential for its implementation in industrial solar cell fabrication processes.

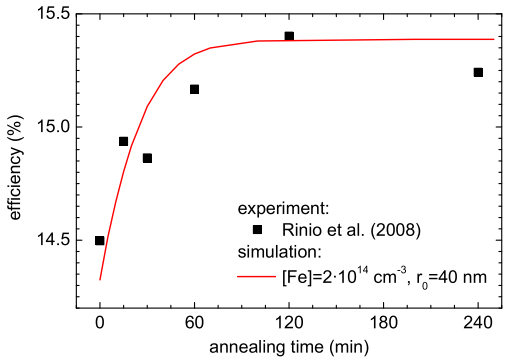


**Figure 1** Solar cell efficiencies for different durations of low-temperature annealing at 500 °C after PD by Rinio *et al.* [5] as dots; final simulated efficiency as line

**2 Simulation** We simulated an LTA experiment that was recently carried out by Rinio *et al.* [5]. In their experiment, solar cells were made out of edge wafers from a p-type mc-Si ingot where Fe is presumed to be the principal lifetime-limiting impurity. After P emitter diffusion at 900 °C for about 10 min, the wafers were subjected to LTA at 500 °C for different times ranging from 15 min up to 4 h.

As the total initial [Fe] as well as the distribution of Fe are unknown, a total concentration of [Fe] = $2{\cdot}10^{14}$ cm$^{-3}$ [7] and a typical mean initial precipitate radius of $r_0 = 40$ nm [8] were assumed as input parameters for our I2E simulator. This leads to a precipitate density of $N = 2.8{\cdot}10^7$cm$^{-3}$ when the relation $N = [\mathrm{Fe}_p]{\cdot}V_{Fe}/(\frac{4}{3}\pi r_0^3)$ between precipitate radius and density is assumed. Here, [Fe$_p$] is the precipitated Fe concentration and $V_{Fe}$ is the volume of the primitive cell in $\beta$-FeSi$_2$ containing one Fe atom.

In Fig. 1, Rinio's experimental data as well as the simulated solar cell efficiency as a function of annealing time are shown. Too many input parameters are unknown to perform truly quantitative simulations. Nevertheless, an important trend in the efficiency improvement due to LTA can be observed: more than 90% of the efficiency increase occurs during the first 60 min of LTA at 500 °C. According to our model calculations, this increase is due to the reduction of [Fe$_i$] in the bulk, much of it having been gettered to the P-rich layer, in agreement with experimental results [5,9]. For longer annealing times, even for a complete removal of Fe$_i$, a further efficiency increase is inhibited by recombination at FeSi$_2$ precipitates.

To find the optimum temperature for LTA after PD, we calculated the final [Fe$_i$] as a function of the annealing temperature, $T_{LTA}$, for different annealing durations. The calculated curves are shown in Fig. 2a. It is observed that the optimum $T_{LTA}$ for which the final [Fe$_i$] in the bulk reaches its minimum, depends on the annealing duration. The shorter the annealing time, the higher is the optimum $T_{LTA}$. The reduction of [Fe$_i$] by means of external gettering is mainly limited by two mechanisms: at high temperatures [Fe$_i$] is determined by the solid solubility of Fe in Si, $S_{Fe}(T)$, while at low temperatures the Fe$_i$ extraction is limited by the Fe$_i$ diffusivity, $D_{Fe}(T)$. Both parameters, $S_{Fe}(T)$ and $D_{Fe}(T)$, decrease exponentially with decreasing temperature. While [Fe$_i$]$< S_{Fe}(T)$ at a given process temperature, the dissolution of Fe-containing precipitates tends to increase [Fe$_i$] up to the solid solubility limit. At the same time, the diffusion of Fe$_i$ atoms to the P-diffused wafer surface leads to a decrease of [Fe$_i$] in the wafer bulk. The final [Fe$_i$] is determined by the resulting atomic flux towards the P-diffused layer which is related to the product of $S_{Fe}(T) \cdot D_{Fe}(T)$. For any given process time, an optimum temperature exists for which the final [Fe$_i$] reaches a local minimum. For shorter annealing times, a higher $D_{Fe}(T)$ and thus a higher temperature is required so that Fe$_i$ atoms are able to reach the P-diffused near-surface region of the wafer (see Fig. 2a).

The final [Fe$_i$] also depends on the initial distribution of precipitated Fe in the as-grown wafer as shown in Fig. 2b. For a given total Fe concentration of [Fe] = $2{\cdot}10^{14}$ cm$^{-3}$, a high density of small precipitates ($N = 1{\cdot}10^8$ cm$^{-3}$ and $r_0 = 26$ nm) leads to a higher final [Fe$_i$] (solid line) than a lower density of larger precipitates ($N = 2{\cdot}10^7$ cm$^{-3}$ and $r_0 = 45$ nm) (dashed line). This is because for a higher density of small precipitates, the interface area between the precipitate and the Si matrix is larger, so that precipitate dissolution is faster. The same argument holds for the dependence of the final [Fe$_i$] on the total [Fe], also shown in Fig. 2b. For a given precipitate density of $N = 2{\cdot}10^7$ cm$^{-3}$, a lower final [Fe$_i$] is achieved for a low [Fe] of $3{\cdot}10^{13}$ cm$^{-3}$ (dotted line) than for a high [Fe] of $2{\cdot}10^{14}$ cm$^{-3}$ (dashed line).

**3 Experimental** Two sets of p-type mc-Si sister wafers, 11 wafers of grain type A and 6 slightly thicker wafers of grain type B, were chemically polished and cleaned. The wafer thickness after chemical polishing was $d = 240$ µm for sample set A and $d = 260$ µm for sample set B. The resistivities of all samples was about 1.1 $\Omega$cm. All wafers were SiN$_x$-coated on both sides for surface passivation. The as-grown electron lifetime was measured by means of Quasi Steady-State Photoconductance (QSSPC) and lifetime mappings were recorded using µ-Photoconductance Decay (µ-PCD). The concentration of interstitial Fe, [Fe$_i$], was measured via Fe-B pair dissociation [10].

Two wafers (A1 and B1), one of each set, were subjected to PD at 850 °C during 20 min; those will be referred to as reference samples in the following. The other wafers were subjected to PD at 850 °C during 20 min followed by LTA during 15 min close to the inlet of the furnace at temperatures between 550 and 750 °C. Subsequently, the P emitter was etched off, wafers were cleaned again, SiN$_x$-coated on both sides and, finally, the resulting electron lifetime, lifetime mappings and final [Fe$_i$] were measured.

 

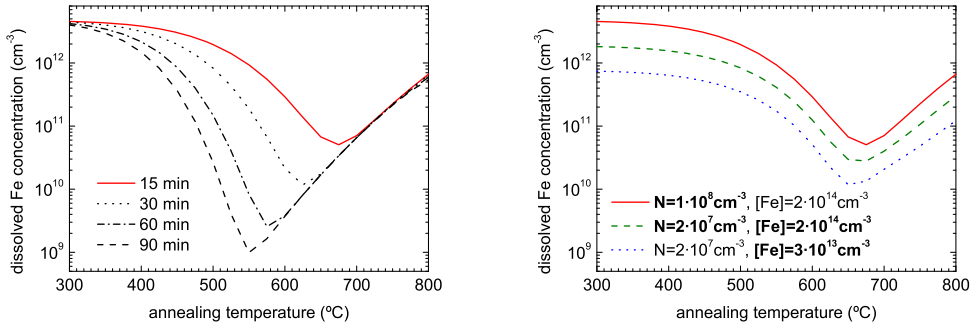


a) b)

**Figure 2** Final dissolved Fe concentrations as a function of $T_{LTA}$ after 10 min PD at 900 °C for (a) different process durations and (b) different as-grown Fe contents and distributions

**4 Experimental results** The final measured [$Fe_i$] for the two different sample sets, respectively, are shown in Fig. 3a as dots. As the temperature during LTA is not well controlled, a mean value of the measured [$Fe_i$] is calculated for the two different temperature ranges $\Delta T$, which are represented by error bars in $x$-direction. Error bars in $y$-direction represent the standard deviations of the mean measured [$Fe_i$] values. The values at $T = 0$°C correspond to [$Fe_i$] measured on the reference samples.

To contrast experimental results with simulations, we calculated [$Fe_i$] as a function of $T_{LTA}$ for the two different sample thicknesses $d = 240$ µm (dashed line) and $d = 260$ µm (dash-dotted line) and the resulting curves are also shown in Fig. 3a. The total as-grown Fe concentration and distribution are unknown so that typical values of [Fe] = $2{\cdot}10^{14}$ cm$^{-3}$ and a precipitate density of $N = 2{\cdot}10^{7}$ cm$^{-3}$ were assumed to fit the experimental data [6–8]. A minimum of [$Fe_i$] is calculated at around 675 °C. Furthermore, the simulations predict a lower final [$Fe_i$] on thinner wafers at temperatures where the Fe extraction is limited by the Fe diffusivity.

In Fig. 3b, the mean lifetime values measured by means of QSSPC on reference samples and on LT annealed samples are plotted as dots. The simulated [$Fe_i$] curves were translated into electron lifetime and are also shown in Fig. 3b. Only the recombination at Fe-B pairs and at $FeSi_2$ precipitates was taken into account. The lifetime maxima are calculated for $T_{LTA}$ around 675 °C corresponding to the minima in [$Fe_i$].

**5 Discussion** Quantitative simulations would require a chemical analysis of the total [Fe] and the determination of the precipitated Fe distribution by means of µ-X-ray analysis [11] as input parameters for the I2E model. Those parameters are unknown in the present wafers so that the experimental data points cannot be all well-fit by the simulated curves. Up to date, the experimental data is insufficient to confirm the existence of the calculated optimum temperature around 675 °C for a 15 min LTA after PD. However, as a proof of concept, it is observed that this *short-tail extended* PD can decrease [$Fe_i$] below $10^{11}$ cm$^{-3}$ and increase the electron lifetime noticeably at temperatures around 600 °C.

For LTA at temperatures below 400 °C, no reduction of [$Fe_i$] is expected as $Fe_i$ in Si is almost immobile at such low temperatures. Therefore, the simulated [$Fe_i$] value at 400 °C corresponds to the simulated value for standard gettering during 20 min PD. In contrast, for temperatures $\gtrsim$700 °C, the gettering efficiency is limited by the dissolution of remaining precipitates which tends to increase [$Fe_i$] in highly Fe-contaminated wafers as mentioned before (see Fig.2). This simulation result is confirmed by the experimental data measured after LTA treatments between 720 and 770 °C. LTA in this temperature range does not reduce the final [$Fe_i$] values as much as LTA in the lower temperature range around 600 °C.

A strong influence of the wafer thickness on the gettering efficiency during LTA is predicted by the simulation. Especially at low temperatures where the efficiency of external gettering is limited by the diffusivity of $Fe_i$, a short LTA treatment will be more efficient, the thinner the wafer is. This effect seems to be reflected in the measured data as well: The final bulk [$Fe_i$] values measured on thinner wafers of type A are slightly lower than those measured on wafers of type B.

Experimental lifetimes on LT annealed samples are somewhat lower than the calculated ones, especially for wafer group B. After removal of interstitial Fe, the electron lifetime seems to be limited by other defects not considered in our calculation. Furthermore, the electron lifetime in wafer set B does not improve to the same amount as in wafer set A. In µ-PCD lifetime mappings (not shown here), areas of very low lifetime were observed on as-grown B wafers which do not improve during gettering treatments.

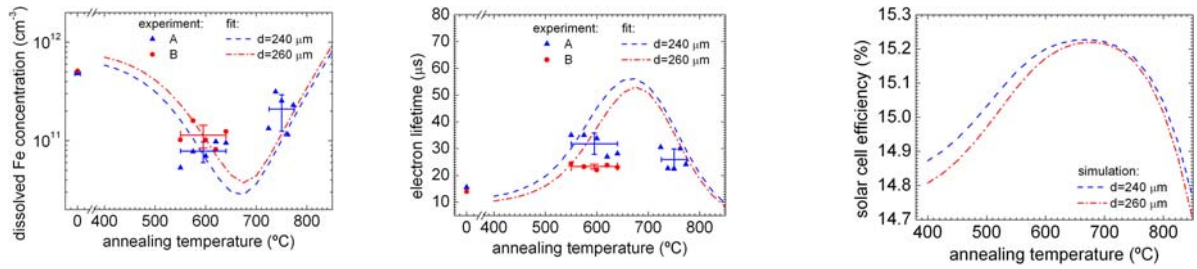


a) Final interstitial Fe concentration b) Final electron lifetime c) Simulated solar cell efficiency

**Figure 3** Measured values of (a) interstitial Fe concentration and (b) electron lifetime on reference samples (corresponding to $T = 0°C$) and on samples subjected to 15 min LTA at different temperatures for wafer set A (triangles) and B (circles). Lines are simulations of (a) final $[Fe_i]$, (b) electron lifetimes and (c) solar cell efficiencies for wafer thickness $d = 240$ µm (dashed line) and $d = 260$ µm (dash-dotted line)

This poor response of low lifetime areas to PD is assumed to be due to high dislocation densities and their interaction with metallic impurities in these areas [12]. Thus, Fe-contaminated wafers containing large areas of high dislocation densities are not expected to improve considerably during LTA.

To quantify the effect of a *short-tail extended* PDG on solar cell performance, the calculated minority carrier lifetimes as a function of $T_{LTA}$ were translated into solar cell efficiencies. Typical solar cell parameters resulting from a standard industrial fabrication process were assumed and solar cell efficiencies for the two different wafer thicknesses, $d = 240$ µm and 260 µm, were calculated. The resulting efficiency curves are shown in Fig. 3c. For the chosen parameters, the solar cell efficiency is increased by 0.4% absolute in comparison to the standard process when PD is followed by a 15 min LTA at temperatures between 600 and 700 °C. Considering this noticeable efficiency increase, it might be worth substituting the standard industrial P emitter diffusion by a *short-tail extended* PDG for wafers with considerable as-grown Fe contents.

**6 Conclusions and outlook** The optimum temperature for LTA following PD mainly depends on the duration of the annealing step. For a *short-tail extended* PDG, consisting of a standard industrial P-diffusion step followed by 15 min LTA, it lies between 650 and 700 °C as indicated by simulations. First experimental results confirm a reduction of [Fe$_i$] below $10^{11}$ cm$^{-3}$ and a noticeable increase in electron lifetime after 15 min LTA around 600 °C.

In ongoing experiments, the short LTA treatments presented herein are being repeated on highly Fe-contaminated Si samples originating from the border of a commercial mc-Si ingot. For this kind of wafers, an appreciable increase in solar cell performance is expected introducing such a *short-tail extended* PDG into the industrial solar cell process.

**Acknowledgements** This work was partially funded by the Spanish Ministerio de Ciencia e Innovación through Thincells project (TEC2008-06798-C03-02), through U.S. Department of Energy under contract number DE-FG36-09GO19001, and through generous gifts from Doug and Barbara Spreng and the Chesonis Family Foundation. The additional support through the MIT-Spain/La Cambra de Barcelona Seed Fund is gratefully acknowledged.

## References

[1] B. L. Sopori, L. Jastrzebski, and T. Tan, cells, in: 25th IEEE PV Specialists Conference (1996), p. 625.
[2] T. U. Naerland, L. Arnberg, and A. Holt, Prog. Photovolt. Res. Appl. **17**, 289 – 296 (2008).
[3] P. Manshanden and L. Geerligs, Sol. Energy Mater. Sol. Cells **90**, 998–1012 (2006).
[4] M. D. Pickett and T. Buonassisi, Appl. Phys. Lett. **92**, 122103 (2008).
[5] M. Rinio, A. Yodyunyong, S. Keipert-Colberg, Y. P. B. Mouafi, D. Borchert, and A. Montesdeoca-Santana, Prog. Photovolt. Res. Appl., available online (2010).
[6] J. Hofstetter, D. P. Fenning, M. I. Bertoni, J. F. Lelièvre, C. del Cañizo, and T. Buonassisi, Prog. Photovolt. Res. Appl., accepted for publication (July 2010).
[7] D. Macdonald, A. Cuevas, A. Kinomura, and Y. Nakano, analysis, in: Proc. 29th IEEE PVSC, New Orleans, Louisiana (2002), pp. 285–288.
[8] T. Buonassisi, A. Istratov, M. Marcus, B. Lai, Z. Cai, S. Heald, and E. Weber, Nat. Mater. **4**, 676–679 (2005).
[9] J. Hofstetter, J. F. Lelièvre, C. del Cañizo, and A. Luque, Solid State Phenom. **156-158**, 387–393 (2010).
[10] D. H. Macdonald, L. J. Geerligs, and A. Azzizi, J. Appl. Phys. **95**(3), 1021–1028 (2004).
[11] T. Buonassisi, A. A. Istratov, M. Heuer, M. A. Marcus, R. Jonczyk, J. Isenberg, B. Lai, Z. Cai, S. Heald, W. Warta, R. Schindler, G. Willeke, and E. R. Weber, J. Appl. Phys. **97**, 074901,1 – 11 (2005).
[12] A. Bentzen, A. Holt, R. Kopecek, G. Stokkan, J. S. Christensen, and B. G. Svensson, J. Appl. Phys. **99**, 093509 (2006).

 